Boundary effects and material behavior of Rammed Earth Construction

Geethanjali Kutturu

Bachelor of Engineering, Jawaharlal Nehru Technological University, 2013

A Report Submitted in Partial Fulfillment of

the Requirements for the Degree of

MASTER OF ENGINEERING

in the Department of Mechanical Engineering

University of Victoria

Boundary effects and material behavior of Rammed Earth Construction

by

Geethanjali Kutturu
Bachelor of Engineering, Jawaharlal Nehru Technological University, 2013

Supervisory Committee

Dr. Rishi Gupta, **Supervisor**
Department of Civil Engineering

Dr. Caterina Valeo, **Departmental Member**
Department of Mechanical Engineering

Abstract

Rammed earth (RE) is the ancient method of construction which is revived in modern days construction due to its sustainability, longevity, low material transportation costs etc., The current study is conducted to predict the boundary effects due to compaction with different ramming heads and to determine the effect of change in constituents on the material properties by non-destructive tests and destructive tests by Schmidt Rebound hammer, UPV (Ultrasonic Pulse Velocity) testing, IR Camera (Infrared Camera), uniaxial compression testing, flexural testing. Cylindrical and prism specimens of different mix designs are subjected to accelerated wetting and drying cycles creating the weatherability effect and reduction in compression strength is measured and prisms are tested to determine the modulus of rupture. This addresses the quality and life of SRE (Stabilized Rammed Earth) and adoption of certain techniques and rammers with different ramming heads to withstand to cold climatic conditions. Also study on First People's House, located at the University of Victoria in British Columbia, provided insight into compressive strength and insulation effects of thermally insulated RE walls after 9 years of natural weathering.

Nomenclature

FPH – First people's House

L - Path length (cm)

MPa - Megapascal

Mix 1 - No Cement removal

Mix 2 - Replacing 15% of cement with 7.5% metakaolin and 7.5% of Fly-ash to the mixture.

NDT - Non -Destructive test

p - Max. applied load,

RE – Rammed Earth

Rich Mix - soil stabilized with high cement content
S - max. stress on tension face,

Second Mix - soil stabilized with low cement content

SRE – Stabilized Rammed Earth

t - Transit time (μs)

UPV – Ultrasonic Pulse velocity

V - Pulse velocity (kms/s)

t - Transit time (μs)

μs - Microsecond

μm - Micrometer

Table of Contents

List of Tables

List of Figures

Acknowledgment

I would like to thank everyone who helped me along way to completing this report and I am very grateful to Dr. Rishi Gupta who provided guidance and support through out and finish my degree smoothly. It is extremely wonderful journey which couldn't be any better without my supervisor. In addition, I thank Dr. Rodney Herring and Dr. Elaine Humphrey for motivating me to finish SEM training which is a great addition to my report.

I am immensely grateful to Mr. Art Makosinki and Mr. Patrick Chang for providing me assistance during my project work and I also wish to extend my thanks to the Mechanical and Civil Engineering Department Staff for providing support throughout my journey in University of Victoria.

Special gratitude goes out to Dr. Armando Tura and Mr. Mathew Walker for their willingness and continuous support and special thanks to Boyu wang and my friends of Civil Engineering Research Group for their help and support and making it more joyous.

I would also like to thank my parents Srinivas Rao, Madhavi and my sister Padmini, husband Sergio Barahona-Salinas for their patience unconditional love and encouragement and very special thanks to my new born son Sergio Naksh Barahona-Salinas who have brought lots of happiness and granted me extra patience and special qualities that helped me become a good mother parallel to being astudent.

Dedication

With all the love in my heart I would like to dedicate this to my dearest parents and sister and to my heart and soul Sergio Fidel Lautaro Barahona-Salinas and my mini me Sergio E. Naksh Barahona-Salinas.

Chapter 1 Introduction

1.1 Overview

Rammed earth (RE) is an ancient method of construction that has been revived during recent times for its sustainability using locally available material such as earth (sand, clay and gravel etc.,). For stabilization of RE, cement or lime [1] is used and such type of construction is known as Stabilized Rammed Earth construction (SRE) which is developed by compacting moist earth mixed with additives (Cement), between the form work, with the rammer. According to some authors [2] RE construction dates to 7500BC the ancient times where man is always moving to a new place and constructing for his shelter and transportation of material is considered as non-ideal due to short stay in a place and RE construction evolves from the "puddled" construction and moving to different parts of the world with successful tradition. This type of construction is also known as Pisé (de terre) in french, and is introduced to eastern seaboard of United States during 1800's [3].

The traditional RE construction has its advantages over steel framed cement construction in reducing total energy costs, production costs and emissions by providing buffering between outside temperature to the humidity levels of indoor space, also, due to installation of thermal insulation and by reducing non-renewable resources as well as transportation costs and cement content in construction process respectively [4]. Some of the ancient RE construction models which are still existent in twenty first century is Great wall of china (3000 years) reflecting its structural stability and few construction models of Canada include St. Thomas Anglican church, Ontario (1841), façade of the Nk'Mip Desert Cultural Centre in Osoyoos, southern British Columbia (largest insulated RE wall of North America) [1].

1.2 Project Motivation

Structural performance of the SRE wall is not fully understood and the design parameters including material characteristics and the associated statistical variation of such engineered walls is not available. To address the need and to standardize the process of molding specimens to determine compressive and flexural characteristics of the materials and to understand the boundary effects of ramming some of the samples have aggregates like metakaolin and fly-ash in different proportions that helps in identifying the modulus of elasticity in compression, tension and bending.

Two test variables – 3″ head rammer and 6″ head rammer are used for the construction of wall and the hardened wall undergoes non-destructive tests (NDT) using Schmidt hammer and Ultrasonic Pulse Velocity tester (UPV) which helps in understanding the properties and homogeneity of the boundary layer of the material. The wall is exposed to natural weathering process and NDT results are taken after 4 months and some samples of the wall are taken for structure analysis likes cracks and voids by using scanning electron microscope (SEM).

One such construction that is present at UVic is First peoples house (FPH) which is constructed in 2008 has undergone almost a decade of natural weathering process. The first article on FPH "Current State of Modern Rammed Earth Construction: A Case study of First Peoples House after Seven Years Exposure" by Allan Kailey and Dr. Rishi Gupta gives an insight about the condition of the FPH walls that underwent 7 years of environmental weathering, Thermal insulation and maintenance strategy for UVic facilities management. Further analysis concerning the sustainability of RE walls to natural weathering and exposing its structural stability after 9 years of FPH wall construction that helps understand the transition over the years and to provide basis for future SRE construction technology.

1.3 Literature review:

Rammed earth constructions around the world have given good service over many centuries and the structure and design of the wall can be enhanced by the type of formwork used during the construction. This type of construction has most of the advantages like lessening the energy consumption due to use of on-site material, inexpensive raw material and its transportation. Cement is used to stabilize the RE which increases strength and durability of RE construction and to test the strength of the RE construction non-destructive and destructive tests are performed by few others like Liang et al [5]. Strength of the stabilized RE construction is depicted in this report and is compared with samples of 2 mix designs one of which is cement stabilization and the other is the addition of industrial wastes like fly-ash and metakaolin.

The Desert Living Center (Las Vegas) [6] aims to provide Nevada residents with information on sustainable living. Canadian architect, Ostrowski, discussed about the ecological footprints of Hakka Buildings in his research. However, people have underestimated this construction in terms of its strength [7].

The non-destructive tests and destructive tests are carried out on RE constructions and several papers are released focusing on compressive strength, insulation etc., Allan Kailey and Rishi Gupta [1] have researched and documented about First peoples' house, University of Victoria which depicts the information on compressive strength, thermal profile and insulation of the walls that are exposed to 7 years of natural weathering and that data is used for comparison with the data obtained after 9 years of natural weathering of FPH walls in this report.

Chapter 2 Experimental Investigation

2.1 Construction Material / Equipment

2.1.1 Rammer:

There are two types of rammers; Manual operated Rammers and Pneumatically Powered Rammers. Now-a-days pneumatic rammers are used for its ease of use and is driven by compressed air which is supplied by the air compressor. The hose is connected to the rammer and air compressor and the motor uses compressed air to develop pressure that start rammers to work as shown in figure 1.

Figure 1: Pneumatically powered rammer connected to the compressor with hoses

Rammers tend to have different ramming heads that vary in size and shape and will affect the boundary conditions. To understand those properties and homogeneity of the boundary layer, rammers with 3″ and 6″ ramming head are used to tamp the aggregate mixture layer by layer and approximately 70 pounds per equal inch of constant air pressure for tamping is necessary for air-tamping.

2.1.2 Formwork:

Formwork is the set of panels that holds the ramming mixture in place incorporating its shape to the wall and surface design on the sides of the wall. It is modelled by using plywood, supporting wooden railings, threaded bars, washer and nuts.

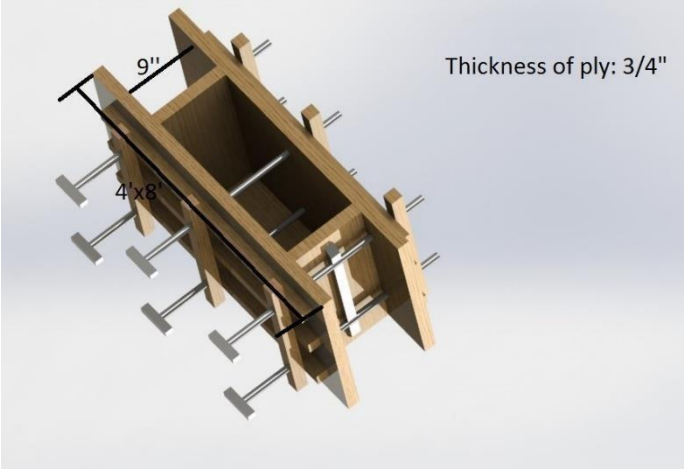

Figure 2: 3-Dimensional image of formwork

In constructing the formwork, plywood of 3/4″ thickness is used and formwork with dimensions

4′x8′x9″ in height, width and breadth respectively is developed and 3-D image is shown in figure 2 and the constructed plywood formwork is shown in figure 3.

Figure 3: 3/4″ thickness Plywood formwork

2.1.3 Cylindrical molds:

Metallic molds are used in constructing cylindrical specimens of dimensions 6″x12″ in diameter and height respectively and are shown as in figure 4.

The Cylindrical specimen is constructed by adding different aggregate mixtures into the molds and ramming it.

These specimens undergo wetting and drying cycles and exposed to ambient air before processing them for compression testing.

Figure 4: Metallic Cylindrical molds

2.1.4 Prism molds:

Plywood of 3/4″ thickness is used in constructing prism molds of 6″x6″x21″ dimensions, height, width and length respectively and is shown as in figure 5a and has similar mix as cylinders.

Ramming mixture of different mix designs are introduced into the molds and re-bar is placed half way through the construction and these prism specimens undergo constant wetting and drying cycles and then exposed to natural weathering process

before used for flexural testing and prism with re-bar introduction while construction is shown in figure 5b.

Figure 5a: plywood based prism molds

Figure 5b: Placement of re-bar in the prism

2.2 Aggregates

Portland cement is most widely used construction material that contributes to major CO_2 emissions as well as greenhouse effect and global warming. To reduce these effects, industrial wastes and by-products are used to replace by some percentage of total weight of Portland cement. Aggregates for RE construction is the mixture of sand, clay and gravel mixed with 8% - 10% of it's weight with water and cement is added as stabilizer at the rate of 3% - 6% by the mixture volume. Therefore, for this construction the mixture of 20mm road base and sand in the ratio of 1:3 with 9% of cement is added to the aggregate mix and 8% of water to the total mix and concrete density of the rammed earth construction is assumed as 2200 kg/m^3

Table 1: Mix designs and material densities in kg/m^3

Material	**Mix1**	**Mix2**
Water	163	163
Cement	168	142.8
Metakaolin	-	12.6
Fly-ash	-	12.6
Aggregate	1868	1868

Therefore, if the aggregate mixture weighs 44 Kgs then 3.96 Kgs of cement is added to the mix and for the mix design 1, since there is no cement removal the total weight of the aggregate mix will be 47.96 Kgs and for mix design 2, 15% of cement is replaced by 7.5% of metakaolin and 7.5% of fly-ash i.e., the aggregate mixture will have 3.37 Kgs of cement and 0.295 Kgs of metakaolin and fly-ash each with total aggregate mixture weight as 47.96 Kgs.

Mix 1: No removal of cement
Mix 2: Replacing 15% of cement with 7.5% metakaolin and 7.5% of Fly-ash to the mixture.

2.2.1 Metakaolin:

Metakaolin is the industrial by-product and is the dehydroxylated form of the clay mineral kaolinite. The thermal dehydroxylation of kaolinite occurs above the temperature range of 500C to 700C and proceeds through progressive amorphization of the crystallites and retains its particle size and morphology until reaction occurs. The formed metakaolin still has 10% of hydroxyls and elimination of those hydroxyls takes place with kinetically more difficult process than dehydroxylation [8].

Portland cement produces concrete mix when replaced with metakaolin (8-20% by total weight). This mix design exhibits properties like increased compressive strength, flexural strength and durability. It also enhances non-shrinkage property due to its particle binding factor, making concrete denser and lessens the pores.

Figure 6: Metakaolin [9]

2.2.2 Fly-ash:

Fly-ash is an industrial waste formed by the combustion of coal. Numerous tons of fly-ash are produced and occupies very large landfill space and to overcome the situation it can be recycled and used as good substitution for Portland cement which in lessens the CO_2 emissions and is cost effective resource.

According to the ASTM standards there are two types of fly-ash classes: class-F and class-C that are suitable to replace Portland cement but it is not only limited to these two types [10]. Class-F is considered as low calcium fly-ash and Class-C is known as high calcium fly-ash with less carbon content (typically <2%). Fly-ash is considered as a non-shrink material and shows greater strengths and workability reducing porosity.

Figure 7: Fly-ash [11]

Chapter 3 Boundary Effects and Homogeneity of RE Wall

RE wall of 4′x8′x9″ in height, width and breadth respectively is constructed by placing the moist mixture of earthen material between the formwork and by ramming the mixture using 3″ and 6″ ramming head rammers. Half section of the wall is rammed using 3″ rammer and the other half with 6″ ramming head to understand the boundary effects and homogeneity of the constructed RE wall.

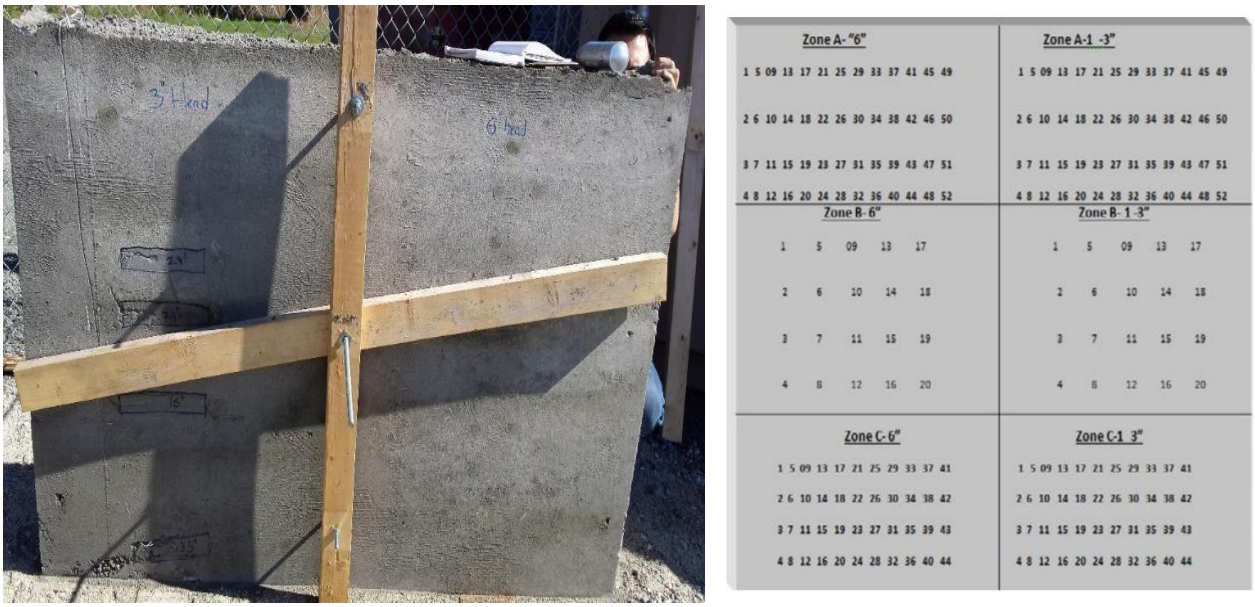

Figure 8: 3" and 6" section of the Rammed Earth wall [16]

To study the boundary effects of the RE wall Schmidt rebound hammer and Ultrasonic pulse velocity (UPV) tester are used which are non-destructive testing methods.

3.1 Schmidt rebound hammer:

Schmidt hammer is used to test the surface hardness of the concretes and to measure the uniaxial compressive strength and young's modulus (E) of rocks and there are two types of hammers: L- and N-type Schmidt hammers that generate different levels of impact energy. N-type hammer is used to test surface hardness of the wall as the uniaxial compressive strength is more than 20 MPa. [12]

The Schmidt hammer is pressed against the wall and then hammer is released and gives a rebound value as the hammer rebounds to obtain the same rebound value at

a point, continuous impacts at a point should be made and peak value must be chosen [12].

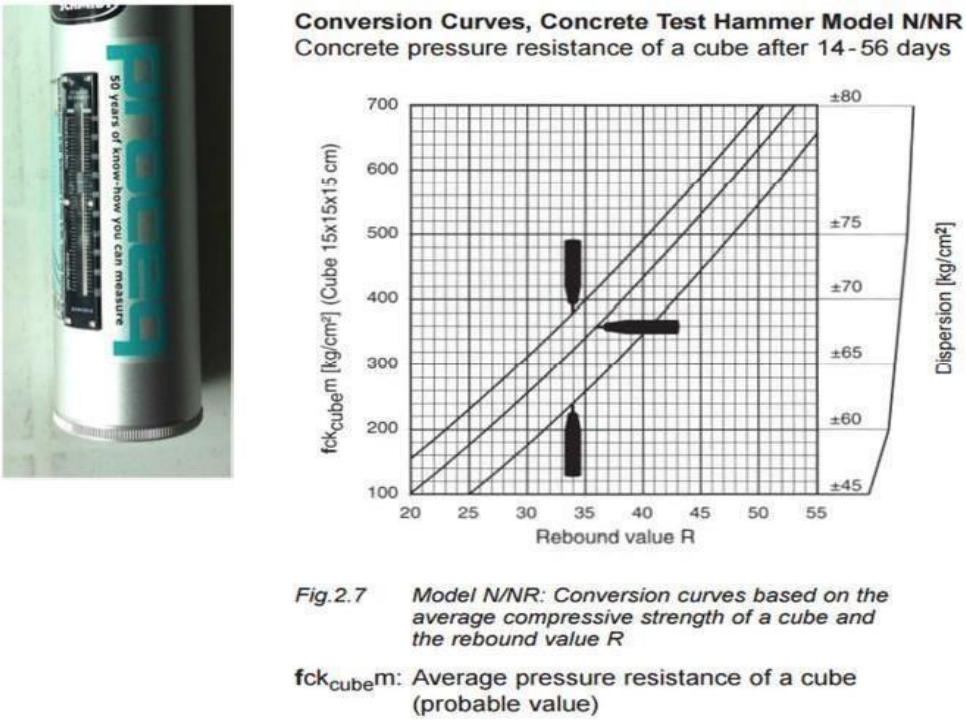

Figure 9: Schmidt rebound hammer and calibration chart [14]

The Compressive strength can be calibrated by obtaining the rebound values (R) and hammer position and then following the curve. Schmidt rebound hammer test on an average of 50 points on top, mid and bottom zones each for 3″ section and 6″ section of the wall and the average compressive strength values that are obtained after 30, 60 and 90 days are calibrated as:

Table 2: Avg. compressive strength [in MPa] of 3" and 6" section of the wall

		30 days		60 days		90 days	
		Mid Section	Corner Section	Mid Section	Corner Section	Mid Section	Corner Section
Wall	3″ Section	52.5	49.5	52.5	50	53	50
	6″ section	46.3	47	47.8	45	49.5	49

The graphical illustration of the compressive strength values of 3″ section and 6″ section of the wall at their mid sections and the corner sections is shown as:

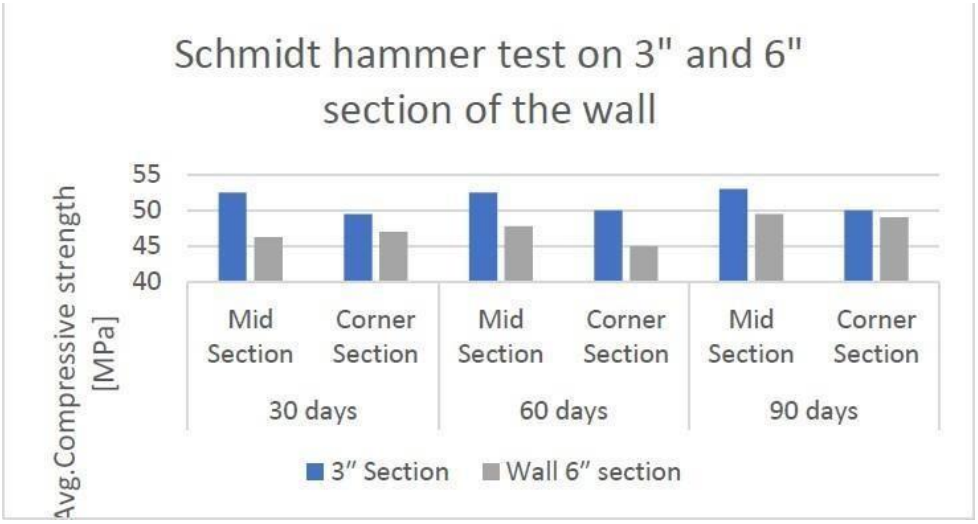

Figure 10: Avg Compressive strength [in MPa] of 3" and 6" section of the RE wall

It was observed that during the 3-month period the 3″ ramming head construction shows higher strength than the 6″ ramming head construction as the ratio of force to area is higher for the 3″ ramming head than the 6″ ramming head construction.

Although 3″ section has higher compressive strength, the strength is not the same at the corner sections (vertical direction) and only has higher strength at mid section (vertical direction) of the wall, this may be due to the shape of the ramming head and being unable to reach the corner sections as a result pressure applied at the corner section is considerably low than at any other sections.

3.2 Ultrasonic Pulse Velocity (UPV):

The UPV tester is used to find the compressive strength by measuring the compressive stress waves travelling through the RE wall and the samples of different mix designs by holding the transducers in: direct, semidirect and indirect ways. The UPV can be used to determine quality and elastic properties [15] of the material medium. The acoustic waves travel from one transducer to the other with a velocity

that is calibrated on it's screen and this velocity defines the compressive strength of the RE, Therefore the pulse velocity can be determined as:

$$V = L/t,$$

Where,

V is Pulse velocity (kms/s),

L is path length (cm) and

t is the transit time (μs).

The UPV test results on RE wall are as follows:

Table 3: UPV [in m/s] test on RE wall

		30 days	60 days	90 days
Wall	3″ Section	4226	4325	4349
	6″ Section	4271	4339	4354

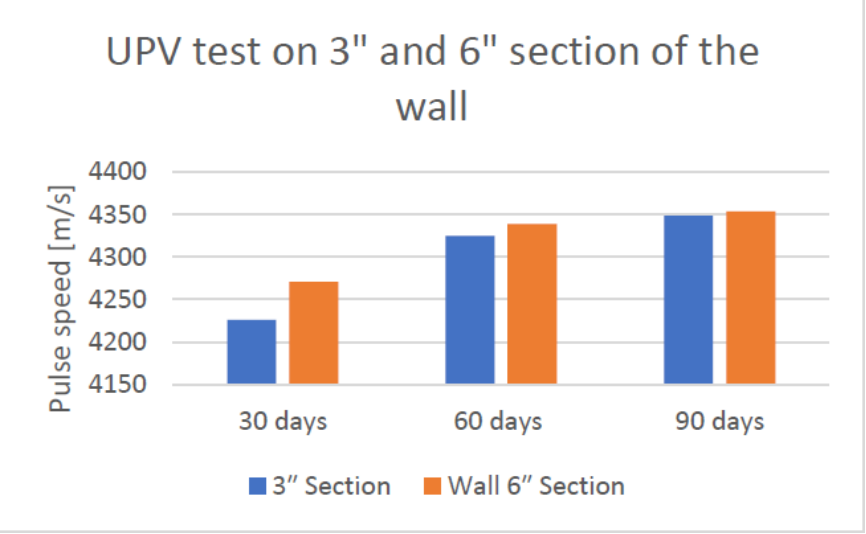

Figure 11: UPV test on 3" and 6" section of the wall

The graph illustrates that the average compression strength is initially slightly lower for the section that is constructed with 3″ head rammer but the strength gradually increased and is almost equal by the end of the tests that were performed after 90 days.

Chapter 4 Destructive Testing to Determine Strength of the Specimens

The results obtained from boundary effects analysis on the wall basis for the molding technique of the specimen and as a result 3″ ramming head rammer is used to construct cylindrical specimens of dimensions 6″x12″ in diameter and height respectively and prism of 6″x6″x21″ dimensions, height, width and length respectively. Also, the re-bars are introduced in the prisms and their interaction is studied during the flexural test of the prism specimens.

Some of these cylindrical and prism specimens are molded with different mix designs and the difference in the specimen strength can be understood. The additives used for the different mix designs include metakaolin and fly-ash. Also, few of these samples have underwent accelerated wetting and drying cycles to imitate the harsh weather conditions.

4.1 Accelerated Wetting & Drying Condition

The two-different destructive testing's that were performed on the RE samples are Compression testing using Forney machine and flexural testing using MTI. Before the test samples were used for testing, they underwent accelerated wetting and drying cycles for a period of two months. Samples were placed in a water tub, cylindrical specimens in one tub and prisms in another tub, a timer is used to pump water from one tub to another tub every six hours as shown in figure 12, so that one of the two tubs are filled with water while the specimens in other tub can dry and this process continued for two months before the samples are taken out to completely dry in the ambient air. This process of wetting and drying is done to imitate harsh weather conditions and reduce the time but have the same impact of weatherability that may be experienced by the RE samples in couple of years.

Figure 12: Prisms and cylinders exposed to accelerated wetting and drying and connected to timer

4.2 Uniaxial Compression Testing:

RE cylindrical specimens are molded and are tested following non-destructive techniques in accordance with ASTM C39 standard. The samples of each mix are tested for their compressive strength by uniaxial compressive test (Forney Machine). For this purpose, 5 samples of Mix 1 and 4 samples of Mix 2 are molded. Of 5 samples of Mix 1 cylindrical RE specimens, 4 samples undergo accelerated wetting and drying cycles and 1 sample is left to rest in ambient weather conditions and of 4 samples of mix 2 RE cylindrical specimens, 2 samples undergo wetting and drying cycles and 2 samples are exposed to ambient weather conditions. i.e.,

Mix 1: No Cement Removal

Wetting & drying: 4 RE samples

Ambient condition: 1 RE samples

Mix 2: 15% cement replacement with 7.5% of Metakaolin and 7.5% of Fly-ash

Wetting & drying: 2 RE samples

Ambient condition: 2 RE samples

The top and bottom side of the cylindrical specimens are smoothened before loading them on to the Forney machine and the specimen specifications are edited such as diameter of the cylinder and length of the cylinder. Now load (compressive load) is noted, when the crack in the specimen is observed as shown in fig 14.

Figure 13: Cylindrical specimen loaded on to Forney machine

The Compressive strength of each specimen of different mix design is obtained by calculating applied load over area of the cylinder the results obtained are as:

Mix 1: No removal of Cement

Mix 2: 15% cement replacement with 7.5% of Metakaolin and 7.5% of Fly-ash

Table 4: Compressive strength of mix 1 at ambient condition and after wetting and drying cycle

Wetting & Drying			Ambient Condition		
Sample No.	Applied Load [N]	Compressive Strength [MPa]	Sample No.	Applied Load [N]	Compressive Strength [MPa]
1	706000	38.73			
2	840527	46.11			
3	663344	36.39			
4	672567	36.89	4	528718	29

Table 5: Compressive strength of mix 2 at ambient condition and after wetting and drying cycle

Wetting & Drying			Ambient Condition		
Sample No.	Applied Load [N]	Compressive Strength [MPa]	Sample No.	Applied Load [N]	Compressive Strength [MPa]
1	588788	32.3	3	677380	37.16
2	627068	34.4	4	631625	34.65

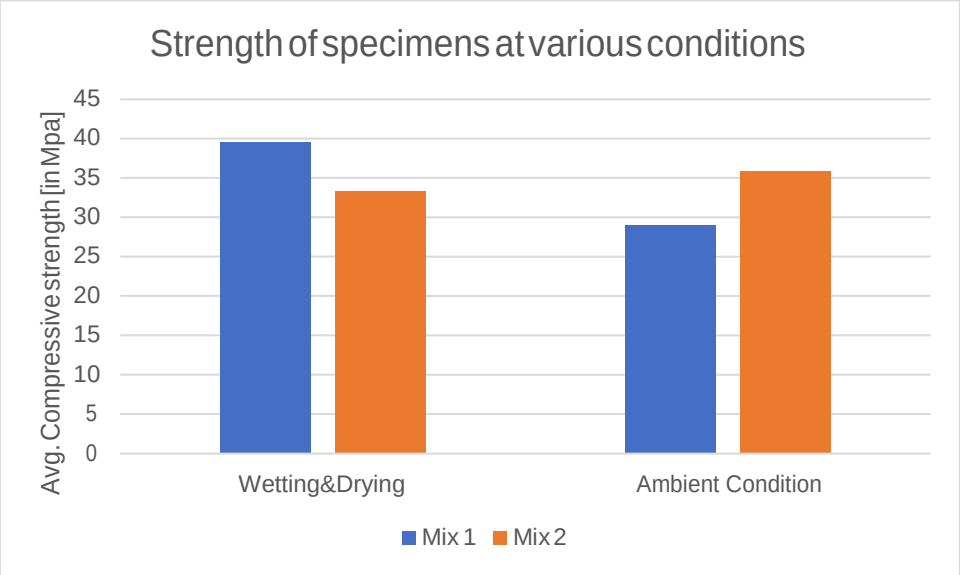

Figure 14: Avg. compressive strengths of mix 1 and mix2 design specimens under different conditions

Under ambient condition mix 2 design shows higher avg. compressive strength than mix 1 as well as the noticeable fact is that the RE compressive strength values fall under the magnitude of concrete compressive strength values [16]. Although the avg. compressive strength values of mix-2 design specimen under ambient condition stands at 35.905 MPa, it decreases to 33.35 MPa when subjected to accelerated wetting and drying conditions. And the avg. compressive strength of mix- 1 design specimens increases from 29 MPa to 39.627 MPa as the cement expands occupying the void space that is available in the RE construction which in turn increases the strength more rapidly. Therefore, the loss of 6.27 MPa of compressive strength under wetting and drying conditions is observed when 15% of cement is replaced by 7.5% Metakaolin and 7.5% Fly-ash

4.3 Flexural Testing:

The Prism samples of Mix 2 design are chosen and simple beam center-point loading test is done in accordance with the ASTM standard C293/C293M – 10. The test samples are subjected to accelerated wetting and drying cycles followed by exposure to natural weatherability for 2 years before testing. Test samples were exposed to rainfall for 24 hours before the flexural testing and the sample surfaces are smoothened on all the sides.

The specimen is loaded on the machine and is supported by two specimen support blocks and center-point loading beam starts to apply load with slower and constant velocity and at loading rate of r = 1200lb/min as shown in figure.

Figure 15: Prism loaded on to MTI machine

Figure 16: Section of prism

Mix 2 samples subjected to flexural strength test and is calculated as shown in the table below:

Table 6: Flexural strength [in MPa] of mix-2 design prisms with rebar

Sample No.	Max. load applied [N]	Modulus of rupture [MPa]
1	33566.6406	7.58
2	49363.6445	11.15

The loading rate is dependent on dimensions of the specimen and is calculated as: $r = 2Sbd^2/3L$ and modulus of rupture is calculated as $R = 3PL/2bd^2$

Where, S= max. stress on tension face, p = Max. applied load, L = Length of the specimen, b = breadth of the specimen and d= depth of the specimen.

Sample 1: Exposed to wetting and drying cycles

For the mix 2 design sample 1, the maximum flexural strength is calibrated as 7.58 MPa .

Sample 2: Exposed to Ambient air

The maximum flexural capacity of mix 2 design, sample 2 is 11.15 MPa.

Chapter 5 SEM Imaging

Aggregate Segmentation from images is essential for determining the porosity of cement stabilized soil samples by SEM image analysis.

5.1 Specimen Preparation

There are 2 types of specimens, rough surface specimens and smooth surface specimens. In this project analysis is done on rough surface specimens which is referred to fractured surfaces.

5.1.1 Drying:

The cementitious material is to be dried before analysis to remove any portions of free water, only when specimen can be stuck to the specimen stub or conductive coating can be done. Therefore, the fractured structure is placed in a vacuum desiccator for at least 48 hours.

The disadvantages of not drying the specimen are, when the specimen is placed in the SEM chamber, the water vapor forms as an obstructing layer on the electron gun resulting in shutdown of the machine.

5.1.2 Conductive coating application:

Concrete specimens are non-conductive and requires a conductive coating ex: Carbon coating, gold coating or gold-palladium coating. While the carbon coating is done in a unit with rotary pump or turbo pump or diffusion pump, Gold or gold-palladium coating is done by sputtering process.

To get superior quality images of the fractured structures specimens are coated with gold by sputtering. The sputtering process coats the sample in random direction and the coating can be done more effectively.

Sputtering is done by placing the specimen in the chamber and by ejecting gold atoms on to it and this coating can be more even and effective when argon gas is passed through the chamber as argon atoms are heavier than oxygen or nitrogen and can randomize path of gold atoms. [17]

5.1.3 Specimen handling:

The dried specimen from the vacuum desiccator is taken and attached to the stub that is covered with conductive carbon paste or double sided conductive carbon/copper adhesive tape can be used to secure the specimen on the stub.

The specimen stub with specimen on it is then placed in the chamber to undergo gold sputtering process and after this process, the specimens are ready to be placed into SEM chamber for analysis.

5.2 ImageJ

ImageJ is the Java-based open-source software which provides the cutting edge in image processing, and is developed by Wayne Rasband. To run this program, the system only needs operating system specific Java run time environment (JRE) and the additional functionality programs are developed like, plugins and macros by some program developers. [18]

Using SEM, images of the fractured samples are taken and analysed using digital image analysis software (ImageJ). The images developed using scanning electron microscope, are of the samples taken from the corners of the wall which underwent ramming with 3-inch diameter head rammer. Two sample specimens are taken from the wall of which one sample is from the top corner which has the rich mix (soil stabilized with high cement content) and the other one from second mix which is below the rich mix surface and has low cement content and shows difference in the strength or surface hardness in those areas.

Image 1: Name of the file: 1 surface_m004.tif Images from SEM (Hitachi S-4800) are stored in .tif format and are used in ImageJ software to check the porosity range of those samples and analyse their surface plots and compare the results in between them.

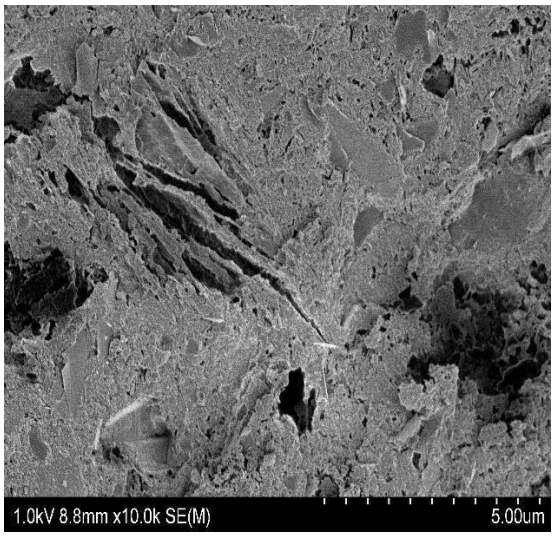

Figure 17: Rich mix sample from SEM image

The SEM image of the sample taken from the top corner of the wall, in which cement

content is high (rich mix) than the soil. From the image, it is hypothesized that the rough surface is cement based material and is also amorphous and porous too and the granular particles or the grain shaped elements are the sand particles.

Due to the compaction, weathering, cement material content etc., and numerous factors, the large cracks and voids are eminent.

5.2.1 Analysis:

ImageJ software is used for the digital image analysis of the SEM image (.tif file)

- The scale is set for the image for analysis. The file is opened in ImageJ and the scale is set based on the measurement that is read on the image. For example, it is 5.00 micrometers for the above image. (Go to analyze and click on set scale)

- Under the analyze button, selecting set measurements and the required elements that are needed to be analyzed are chosen, ex: total area and area fraction of porosity for the above image.

- The image is selected using the rectangle selection and is cropped by clicking on image and crop or Ctrl+shift+X for windows and the area to be analyzed is set.

- Using image option go to adjust and click on threshold and the image threshold can be adjusted by choosing color red or black and white or over and under for green and blue, and for easy identification of voids by thresholding red color ischosen.

- After setting the threshold balance and applying the changes to the image, the image is then ready to be analyzed and click on analyze and go to analyze particles and in the options set it to global and summarize for the result

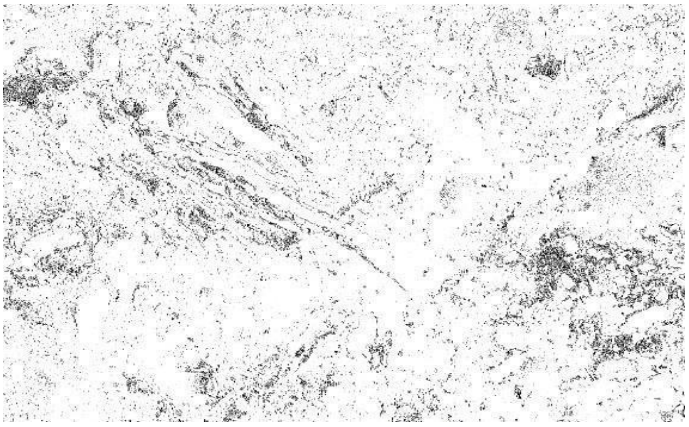

Figure 18: Binary image of rich mix sample

Slice	Count	Total Area	Avg. Size	% Area	Circ.	Solidity
1 surface_m004.tif	62931	6.984	1.110E-4	6.293	0.873	0.890

- By selecting the modified image (after threshold application), and clicking on analyze and plot profile between the gray value and the distance. Gray value gives the information about the voids as the value for black being 0 and white being 255(max).

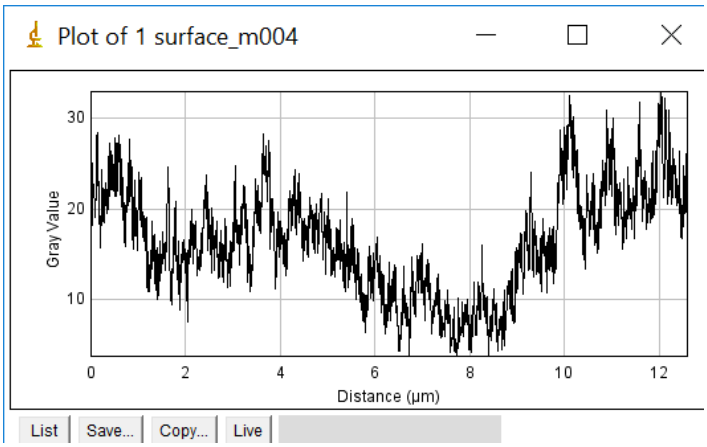

Figure 19: Gray value v/s distance plot of rich mix

- We can also plot the surface or the 3D image of the SEM image that is being analyzed by clicking on analyze and plot surface. The surface of this file is given as:

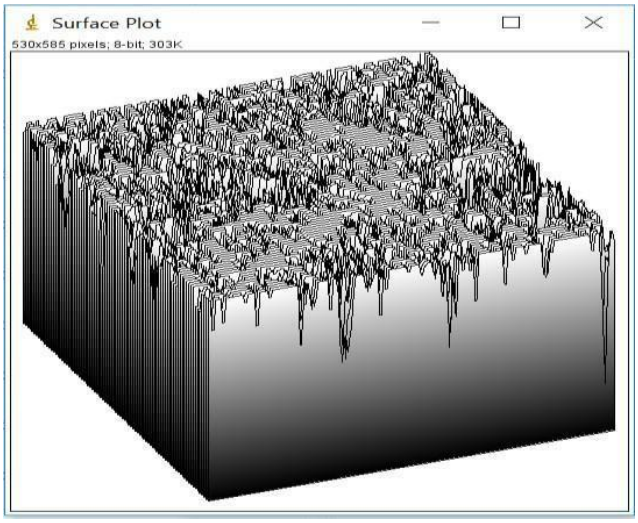

Figure 20: Rich mix 3-Dimensional surface plot

- Additionally, when the image for which threshold settings are applied and analyzed for porosity by clicking on analyze particles, we can also set the settings to show pores in elliptical shape (choose based on requirement) and in the resulting image we can fill those elliptical shaped voids by masking to see the area they covered in an image.

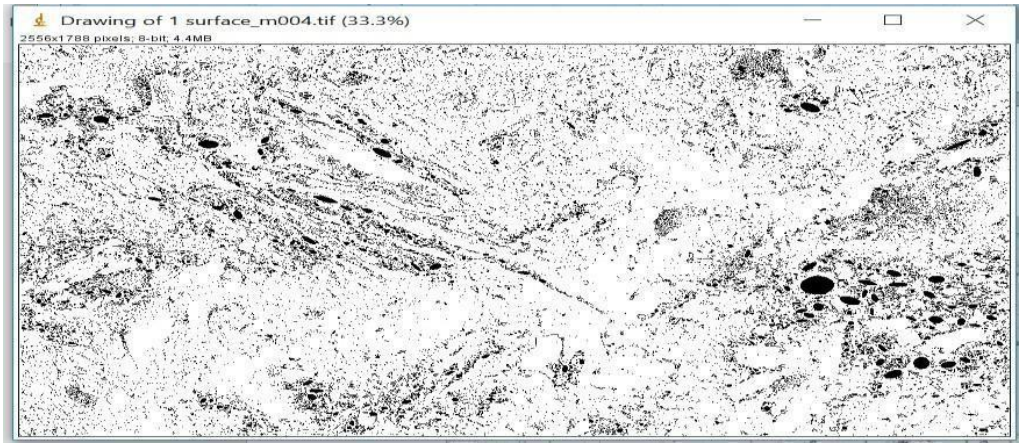

Figure 21: Rich mix - Binary image with pores filled

Similarly, analysis is done for the second file: 5 surface_m010.tif

From the Image processing, it is assumed as, rough surface which is in amorphous phase represents Cementous material and the granular structure represents soil.

Features of this sample includes lower emission current than the sample of rich mix and was emitting charge during SEM imaging.

Figure 22: Sample of other mix

The gray scale image from SEM imaging is now uploaded in the ImageJ software for image analysis. Scale is set to 4.00um for the above image that is to be analyzed

and measurements are set in the software as total area of the sample image and %area of porous content are selected, along with those measurements any additional measurements can also be selected if needed.

Now the image to be processed is selected by using the rectangular box over the image and cropping the image and this process is known as image selection. After Image selection and cropping and applying those settings, image segmentation must be done.

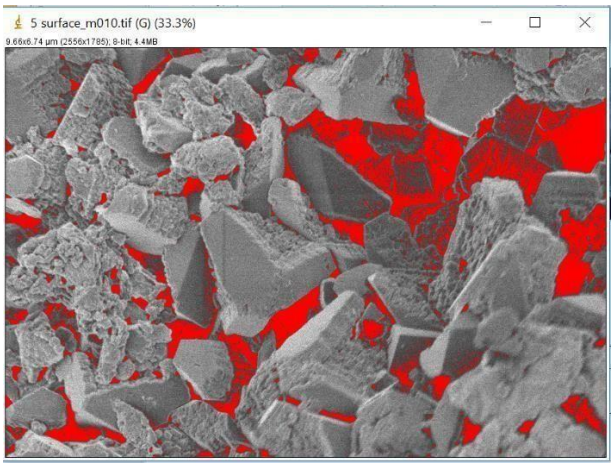

Figure 23: Second mix sample threshold balancing

Image Segmentation is the process of developing the boundaries between diverse types of materials present in the image, it is cementitious material v/s soil v/s pores for this image, this process is also known as thresholding and it is done by highlighting porous area using red color balancing and applying those settings to change the grey scale image to binary image as the software only analyzes binary images and the above image is taken during thresholding process.

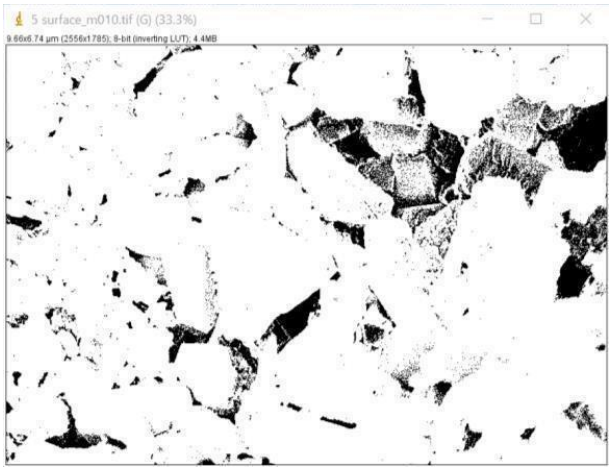

Figure 24: Second mix sample - Binary image

Now, the results are analyzed and summarized results are taken and a graph of grey scale v/s distance is plotted as follows:

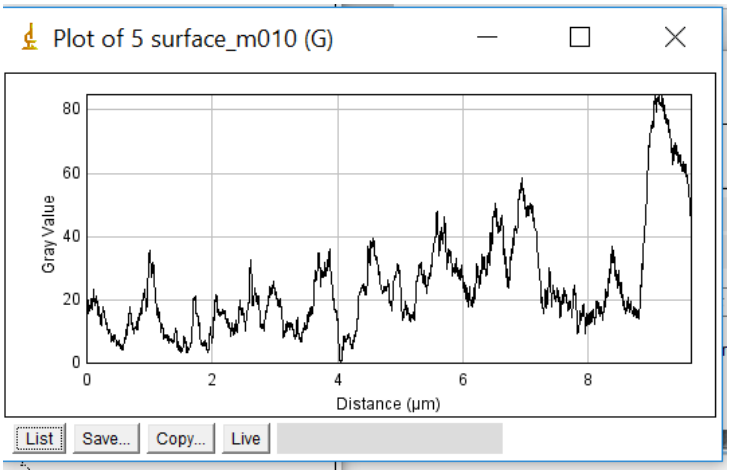

Figure 25: Gray Value v/s distance plot of second mix

The summarized results give us the count for the pores that are present in the image area selected and notifies about the percentage of area that is porous and is as follows:

Slice	Count	Total Area	Avg. Size	% Area	Circ.	Solidity
5 surface_m010.tif	15092	5.562	3.686E-4	8.540	0.896	0.909

8.54% of the total area is porous.

From the results that are obtained, if an imaginary 3D image of the surface with the above-mentioned features is developed, it would be as shown in figure.

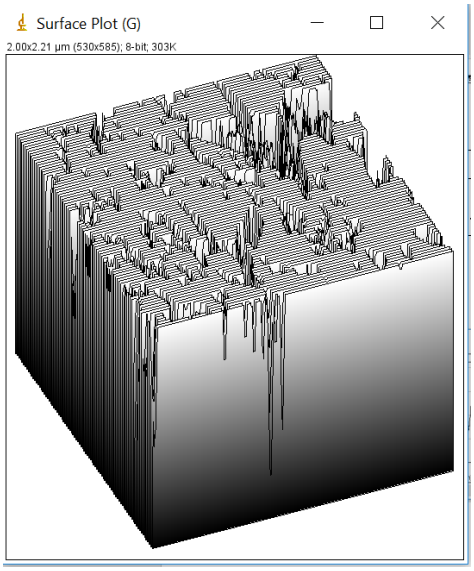

Figure 26: Second mix 3-dimensional surface plot

From the tables, the following is interpreted,

6.29% of the total area (6.984µm^3) of the rich mix (top of the wall) is porous and 8.54% of the total area (5.562µm^3) of the second mix is porous i.e., 0.439µm^3 of area of rich mix and 0.474µm^3 of area of second mix is porous and the ratio of total area to the area of porosity for rich mix is 15.9 and for second mix is 11.73 and is shown in the figure below:

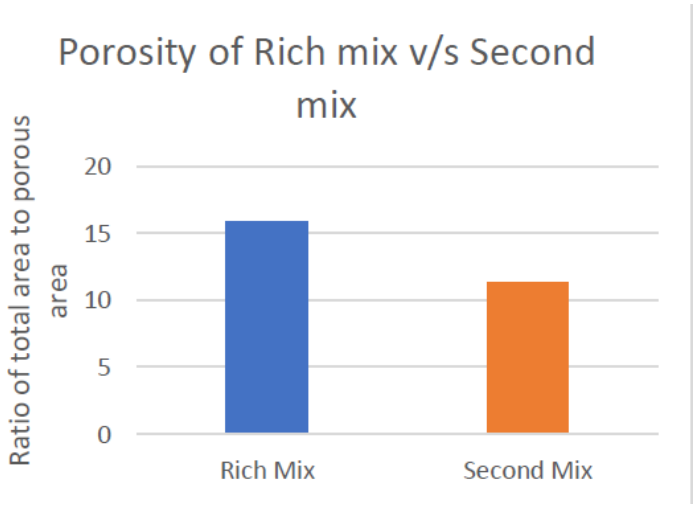

Figure 27: Porosity of Rich mix v/s Second mix

From the above figure, it is understood that rich mix is highly porous than second mix but due to the less cement content and granular particles (soil) orientation in second mix the specimen image portrays its loosely packed structure with less binding properties

Chapter 6 Study on First People's House (UVic)

First People's house is an academic and cultural centre for Indigenous students [19]. The construction began in April 2008 and was completed in August 2009, the main entrance faces east and has the rammed earth wall that is exposed to natural weatherability. Half of the wall 1 is exterior-exterior type and the other is exterior-interior type i.e., half of the other side of the wall 1 is enclosed in a room. The wall 2 which is the rear entrance, facing towards west, is exterior-interior type. Attached to the wall 2 is the storm retention pond where the rain water that hits the roof is passaged towards this pond.

6.1 Schmidt rebound hammer test:

Certain points were marked to determine the compressive test of SRE wall and there are 2 reasons behind choosing those points. 1) to target minimum and equally distributed strength and 2) to compare the results with those that were taken after 7 years of natural weatherability.

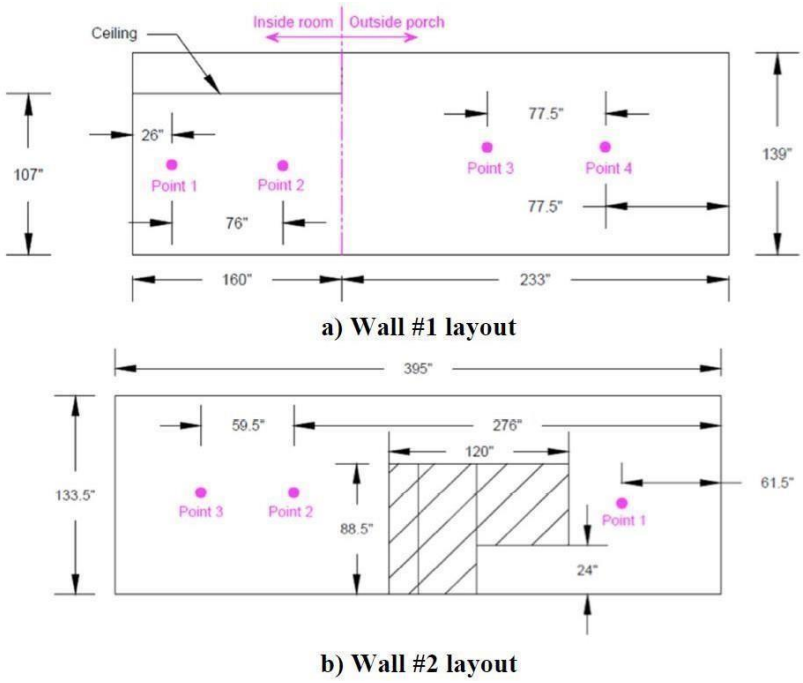

Figure 28: FPH wall layout [1]

Table 7: Interior and exterior avg. rebound values of the FPH wall after 9 years of natural weathering

	Interior				Exterior			
	P1	P2	P3	P4	P1	P2	P3	P4
Wall 1	47.3	39	41.25	38.3	31	25	33.6	36.6
Wall 2	-	-	-	-	38.3	39.3	34.3	-

Table 8: Interior and exterior avg. Compression strength [in MPa] values of the FPH wall after 9 years of natural weathering

	Interior				Exterior			
	P1	P2	P3	P4	P1	P2	P3	P4
Wall 1	56.6	40.6	45.25	39.3	27	17.16	31.5	36.91
Wall 2	-	-	-	-	39.5	41.3	32.5	-

The avg. compression strength results that were taken after 7 years of FPH construction by Allan Kailey and Gupta Rishi is considered to compare the difference in strength between the outside surface and inside surface with the values that were obtained after 9 years of FPH wall exposure to natural weathering.

The difference in compressive strength of wall 1 between the inside and outside surface calculated after 9 years of natural weathering, at point 1,2,3 and 4 are 29.6 MPa, 23.44 MPa, 13.75 MPa, 2.39 MPa respectively. And from Kaileys' [1] the data is gathered as 6.86 MPa, 1.96 MPa, -0.98 MPa and 0.00 MPa at point 1,2,3 and 4 respectively. And the difference of compressive strengths of wall 1 inside and outside surfaces at 9 years and at 7 years period is shown as:

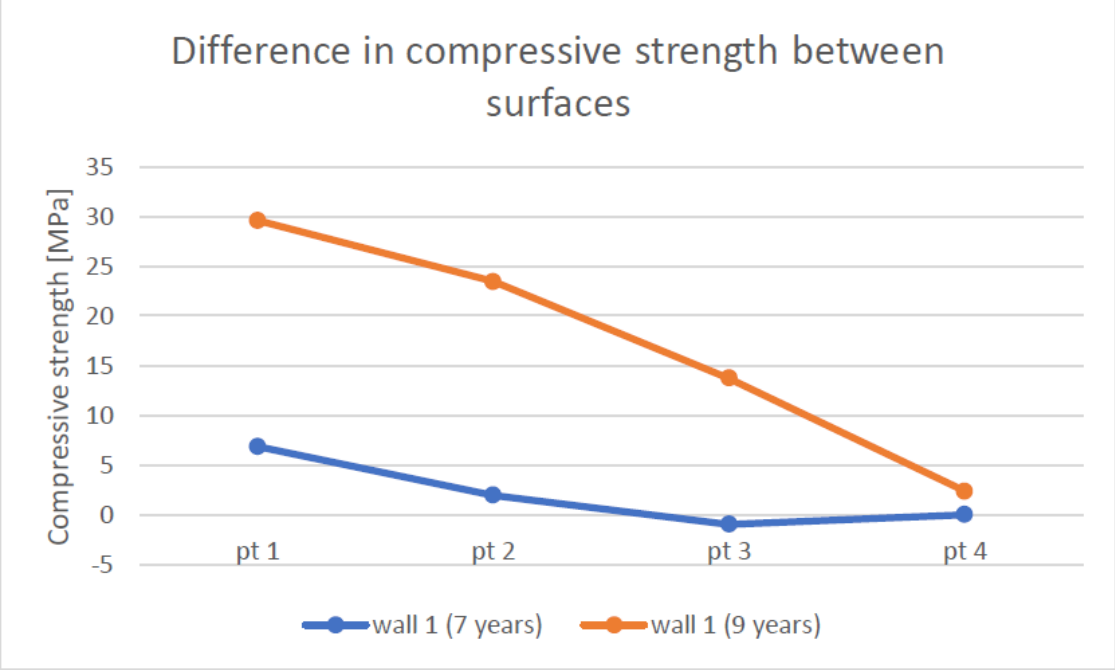

Figure 29: Compressive strength difference between surfaces at 7 years and 9 years

The large compressive strength difference between inside and outside surface of wall 1 calibrated after 9 years of natural weathering is due to the weather conditions (season) on the day of test. The wall 2 strength difference can't be calibrated due to insufficient data.

6.2 InfraRed Camera:

IR camera captures thermal patters of an image and calibrates the emissive power of surfaces at different temperatures [20] and heat loss due to radiation from the surface can be calculated as $q'' = \sigma \varepsilon T^4$.

Where q'' is energy radiated per unit area $\{W/m^2\}$, σ is Stefan-Boltzman constant $\{5.67051 \times 10\text{-}8\ W/m^2K\}$, ε is emissivity {approximately 0.94 for SRE} [1] and T is absolute temperature of the surface {K}

This can be used for non-destructible evaluation of thermal profile of the building and helps identify missing or damaged insulation. To find the thermal profile of RE building, IR camera is used to find temperature of the interior and exterior of the body and calculate the heat loss from the temperature difference between the two sides. Since the heat loss occurred due to conduction, $q_{cond} = U\Delta T$, Where U is the

thermal resistivity which is the reciprocal of thermal resistance, R and its value is estimated to be 0.337 for a wall with 400mm thick insulation and has 50mm thick polyurethane at its centre [4]. Therefore, temperature of the walls at different points on the SRE wall is obtained as shown in table 9 :

Table 9: Interior and exterior temperatures [C] of the FPH wall

	Interior				Exterior			
	P1	P2	P3	P4	P1	P2	P3	P4
Wall 1	22.6	22.8	11.5	11.7	10.3	9.7	10.5	10.2
Wall 2	-	-	-	-	11.3	12.5	12.8	-

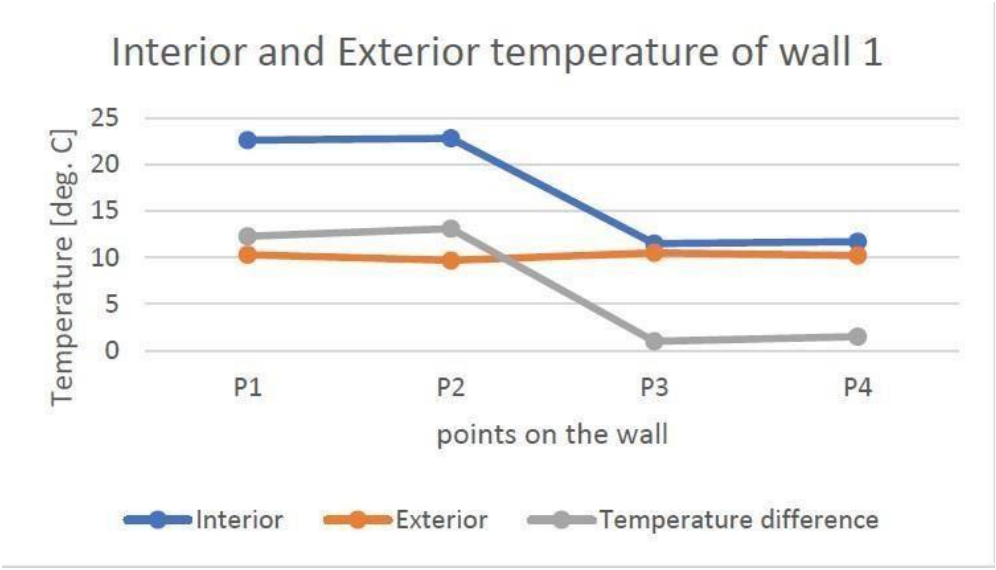

Figure 30: Interior and exterior temperature of wall 1

Heat loss between interior and exterior walls of wall 1 at point 1 and 2 is high, because point 1 and 2 are exposed to different weather conditions on either side unlike point 3 and 4 that are exposed to same weather conditions {U- value 0.339 W/m^2k}

Table 10: Avg. Heat loss [in W/m^2k] between the surfaces of wall 1 of FPH wall

Wall 1	U-Value [W/m^2k]	Temperature Difference [C]	Heat loss [W/m^2k]	Avg. Heat loss [W/m^2k]
Point 1	0.337	12.3	4.14	4.27
Point 2	0.337	13.1	4.41	

The average heat loss between the surfaces of wall 1 after 7 years of exposure to the natural weather is calibrated in Kailey's paper as shown in the table below:

Table 11: Calculated Heat loss [1]

	Point	U-value [W/m^{2}K]	Difference [^{o}C]	Heat loss [W/m^{2}K]	Average heat loss/room [W/^{2}K]
Wall #1	1	0.339	12.1	4.17	4.49
	2	0.339	14.2	4.81	
Wall #2	1	0.339	14.2	4.81	3.42
	2	0.339	9.2	3.08	3.53
	3	0.339	11.8	3.97	

By comparison, it is observed that there is a difference of 0.22 W/m^{2}k in average heat loss between the surfaces of wall 1. Due to insufficient data on wall 2 the average heat loss is not calculated. Also, Hall's [4] theory concludes that high moisture content has negative impact on thermal resistance.

Chapter 7 Conclusion

My contribution for Rammed Earth project include designing and developing of formwork for wall, beams and resourcing re-bars, aggregates, UPV tester, cylindrical molds, rammers, air compressor and constructing wall, cylindrical and beam molds and performing SEM imaging and destructive testing.

SRE is one of the oldest construction method but has no definitive understanding about the structural performance which is addressed and the molding technique of the specimens is understood by performing non-destructive tests using Schmidt rebound hammer and UPV on the RE wall and 3″ head rammer is considered as best suited than 6″ head rammer due to its advantages like high compressive strength than 6″ as well as better compressive strength at corners when compared to 6″ head rammer and this is due to the size of the ramming head to the area of compaction value which is high for 3″ ramming head. However, there are rammers with different ramming head shape and size and show different boundary effects along the formwork

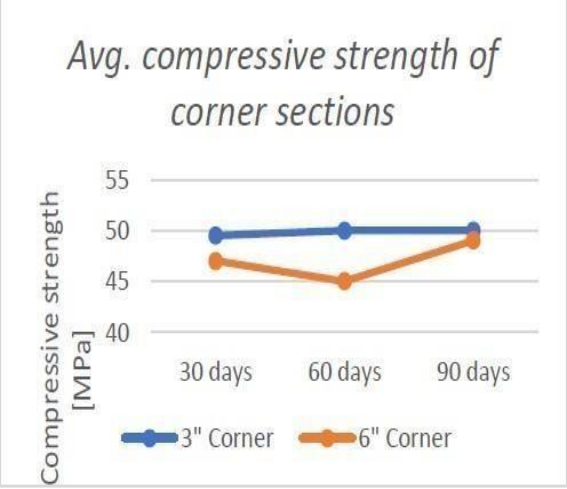

Figure 31: Avg. compressive strength of corner sections

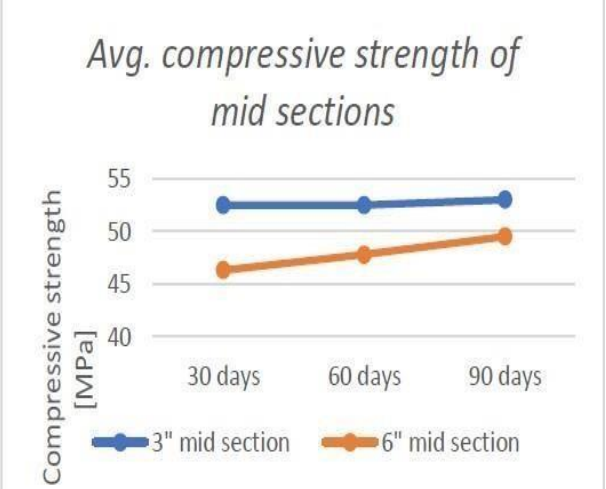

Figure 32: Avg. compressive strength of mid sections

As the 3″ head rammer is concluded to be best for its effect on boundary properties, it is used for constructing cylinders and prisms which are later tested for the compression and bending strength. These specimens are constructed based on two different mix designs one of which replaces cement constituents by 15% with 7.5% of metakaolin and 7.5% of fly-ash and the loss of strength is calibrated as 6.27 MPa when subjected to accelerated wetting and drying conditions and followed by destructive test known as uniaxial compression testing while the average compression strength of the specimens range between 29 MPa and 39 MPa under ambient and wetting and drying conditions and for both mix designs.

Similarly, flexural strength test is carried out using MTI machine to understand the interactions of re-bar while test is in progress and to determine the de-bonding of the rebar. Samples of mix- 2 design are used of which sample 1 is subjected to accelerated wetting and drying conditions and sample is exposed to natural weathering and the flexural strength of samples varied by 3.57 MPa and de-bonding for sample 1 occurs just as the max. stress drops to 40% and for sample 2 it occurs as the stress value drops to 70%, however, the no. of samples that were left to perform flexural strength test is very low and can’t conclude from the available data.

Also, SEM imaging analysis is carried out on the fractured structures of 3″ section of the RE wall. One of those structures is from the top section of the wall which is rich in cement constituent and has 6.29% of the total area as porous and for the second structure 8.54% of the total area is porous in nature. The difference is noted due to the use of cement and its effects, also, due to particle orientation. It is therefore understood that SEM imaging can be used when the morphology of the RE samples is to be studied.

Comparing results of FPH wall after 9 years of weatherability to 7 years weatherability results that are obtained from “Allan Kailey’s” paper [1] explains changes happened to SRE due to weatherability, the avg. heat loss for wall 1 is approximately the same but slightly decreased by 0.46% where as the compression strength results indicate the difference of compressive strengths between inside surfaces and outside surfaces of wall 1 and the tests confirmed that the difference is increased when compared to the results obtained from 7 years of natural weathering. However, the tests are carried out under different weather conditions at both times and this may contribute to the possible differences in the results.

Bibliography

[1] Kailey, A., & Gupta, R. (2016). Current State of Modern Rammed Construction: A Case Study of First Peoples House after Seven Years Exposure. *Key Engineering Materials*, *666*.

[2] Berge, B. (2009). *The ecology of building materials*. Routledge.

[3] McHenry, P. G. (1984). *Adobe and rammed earth buildings: design and construction*. University of Arizona Press.

[4] Hall, M., & Allinson, D. (2009). Assessing the effects of soil grading on the moisture content-dependent thermal conductivity of stabilised rammed earth materials. *Applied Thermal Engineering*, *29*(4), 740-747.

[5] Liang, R., Stanislawski, D., & Hota, G. (2011, October). Structural responses of Hakka rammed earth buildings under earthquake loads. In *Proceedings of International Workshop on Rammed Earth Materials and SustainableStructures*.

[6] Liang, R., Hota, G., Lei, Y., Li, Y., Stanislawski, D., & Jiang, Y. (2013). Nondestructive evaluation of historic Hakka rammed earth structures. *Sustainability*, *5*(1), 298-315.

[7] Liang, R., & Hota, G. (2009). Hakka Tulou and Science. Hakka Tulou Forum: Lessons to Be Learned. *Past, Present and Future, June, 24*.

[8] Bellotto, M., Gualtieri, A., Artioli, G., & Clark, S. M. (1995). Kinetic study of the kaolinite-mullite reaction sequence. Part I: kaolinite dehydroxylation. *Physics and chemistry of minerals*, *22*(4), 207-217.

[9] https://3.imimg.com/data3/LM/HF/MY-4485073/metakaolin-250x250.jpg

[10] Bilodeau, A., & Malhotra, V. M. (2000). High-volume fly ash system: concrete solution for sustainable development. *ACI Materials Journal*, *97*(1), 41-48.

[11] https://www.masterbuilder.co.in/wp-content/uploads/2017/08/Coal-Fly-Ash-Class-F.jpg

[12] Aydin, A., & Basu, A. (2005). The Schmidt hammer in rock material characterization. *Engineering Geology*, *81*(1), 1-14.

[13] Sudin, M. A. S., & Ramli, M. (2014). Effect of Specimen Shape and Size on the Compressive Strength of Foamed Concrete. In *MATEC Web of Conferences* (Vol. 10, p. 02003). EDP Sciences.

[14] Proceq . (2015). *Operating Instructions Original Schmidt.* Retrieved 4 2015, 6, from Proceq: http://www.proceq.com/en/site/downloads/Original%20Schmidt.html

[15] Kewalramani, M. A., & Gupta, R. (2006). Concrete compressive strength prediction using ultrasonic pulse velocity through artificial neural networks. *Automation in Construction*, *15*(3), 374-379.

[16] Khan, A. A. (2017). Determining Material Characteristics of "Rammed Earth" Using Non Destructive Test Methods for Structural Design.

[17] Winter, N. B., & Winter, N. B. (2012). *Scanning electron microscopy of cement and concrete*. WHD Microanalysis.

[18] Collins, T. J. (2007). ImageJ for microscopy. *Biotechniques*, *43*(1 Suppl), 25-30.

[19] University of Victoria. (2008, August). *First Peoples House Brochure.* Retrieved from First Peoples House: http://web.uvic.ca/fphouse/pdf/first-peoples-house-brochure- Aug08.pdf

[20] Balaras, C. A., & Argiriou, A. A. (2002). Infrared thermography for building diagnostics. *Energy and buildings*, *34*(2), 171-183.